

LSD Based Vision Detection System for Industrial Robot under Complex Illumination Conditions

Weiping Liu, Weidong Chen and Ruimin Wu

Abstract— In this paper, we present an object vision detection and localization method approach to the industrial robotic system under complex illumination conditions. In industrial applications of machine vision, many of feature extraction algorithms depend on edge detection, which can be affected by ambient illumination variation and loses efficacy. We propose a robust method that combines image enhancement, edge detection and feature information extraction to detect and locate target components. The key idea is to use a histogram key point constrained homomorphic filtering to enhance the image followed by line and arc segments feature detection. Finally, the experimental results on probe end-face image dataset and steelmaking automation manufacture demonstrate the ability of the proposed method to perform more robust and accurate effectiveness under illumination variant conditions.

I. INTRODUCTION

Recently, vision-based guidance of robotic arms has received much attention, especially in industrial machine vision applications [1]. The previous work mainly focuses on the feasibility and stability of the system, however, for some specific applications such as steelmaking automation manufacture, the ambient illumination can be complicated and therefore increases the difficulty for object detection.

Since improvement of the illumination robustness is a difficult problem, some methods are directly or indirectly extract illumination invariant information such as multiscale retinex [2] and discrete cosine transform based normalization technique [3], most of them are sensitive to illumination variation and easy to lose detail information. Yu et al. [4] proposed a method for view and illumination invariant image matching which estimates the relationship of the relative view and illumination of the images iteratively, but this method needs paired reference initial image for matching.

Another image processing technique designed to restore the degraded images is homomorphic filtering (HF) [5], HF enhances and restores the degraded images under uneven illumination condition by simultaneously normalizes the brightness across an image and increases contrast, however, may not appropriate to deal with the fake information caused

W. Liu and W. Chen are with Department of Automation, Shanghai Jiao Tong University and Key Laboratory of System Control and Information Processing, Ministry of Education of China. R. Wu is with R&D Center, Baoshan Iron & Steel Co. Ltd.. W. Chen is the corresponding author (wdchen@sjtu.edu.cn).

This work is supported by the National Key R&D Program of China under grant 2017YFB1303600.

by high illumination conditions.

For local feature detection, Canny edge detector [6] followed by Hough transform (HT) [7] is used to detect line segments, however HT can cause many false detection results for textured regions with a high edge density, while Circle Hough Transform (CHT) [8], Random Sample Consensus (RANSAC) [9] and template matching (TM) [10] for circle detection comprise many unnecessary calculations and perform poor robustness under complex illumination conditions. Another local feature detection methods are based on line segments approximating and circle edge geometric attributes, such as line segment detector with false detection control (LSD) [11] and the method developed by Lu et al. [12] applied to circle detection. LSD based methods mainly detect line or arc support region where the points share roughly the same level-line angle or the points' level-line angles and distributions change like a curve, and followed by segments clustering to fit the feature candidates. However, LSD based methods perform poor robustness under complex illumination conditions since the coherence of contour information may be split and destroyed under this circumstance.

Herein, we propose a vision detection algorithm combines image enhancement, local feature detection and object localization to overcome the adverse effect of complex illumination. The key idea is to use a histogram key point constrained homomorphic filtering to simultaneously normalizes the brightness across an image and increases contrast, applied to both low and high illumination conditions. Then line and arc-support line segment detector are used to extract the edge line segment and arc segment information which are likely to make up line or circle features. Finally, local fragmented line and arc segments are used to generate initial line or circle sets and verified through geometric based constraints to the final results. Applied to the robot, we transfer the results through the eye-to-hand camera calibrated transformation matrix to the robot and then complete the required task.

The rest of this paper is organized as follows. Section II gives the vision based detection system description. In Section III, the vision detection algorithm is presented. Section IV shows the experiments. Section V concludes the paper.

II. VISION BASED DETECTION SYSTEM DESCRIPTION

In this section, the mechanical design and system structure of the vision detection system for the robot steelmaking system are discussed.

A. Mechanical design and architecture

The mechanical structure of vision-based robot steelmaking system mainly consists of four parts, namely, a six-axis industrial robot, the detection system, a magazine for probe storage and a sublance as Fig. 1 shows, in addition, a gripper (Fig. 1(c)) and photoelectric sensor (Fig. 1(d)) are equipped to the robot. Overall, the robot steelmaking system is designed to perform the task that using the gripper tool to pick probes from the magazine depending on the detected and localized results through the detection system, and then attach the probe to the sublance, finally, the probe is carried to steel water to finish the temperature measuring task.

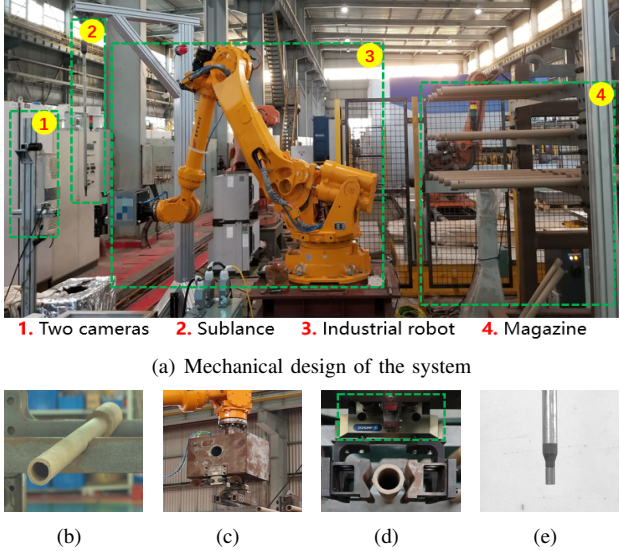


Fig. 1: Mechanical design of the robot steelmaking system. (a) System arrangement. (b) The probe. (c) The gripper installed in the robotic tool. (d) The photoelectric sensor inside the robotic tool. (e) The sublance fixed on the bracket.

B. Vision based detection system structure

Base on the mechanical design and architecture mentioned above, we designed the system structure combines the hardware configurations and software processes.

We divide our system structure coarsely into two parts, namely the mechanical system and vision detection system respectively as Fig. 2 shows. The block of the mechanical system mainly includes the hardware part introduced in the previous section and the robot manipulation part of performing the temperature measuring task. The vision detection system part mainly consists of the optical cameras and the proposed detection algorithm including image enhancement, local feature detection, object localization and information coordinate system conversion.

C. Camera calibration and coordinate system conversion

Camera calibration is an essential step for our system since the position information of the target need to be transformed

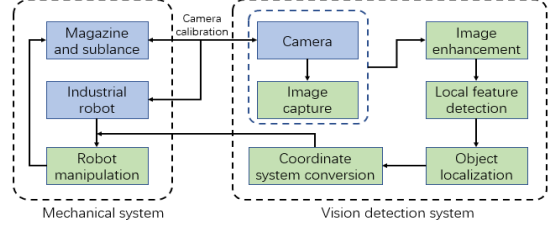


Fig. 2: System structure of the vision based detection system.

to the robot coordinate system. The vision based detection system requires metric information about the environment, so we need to determinate the intrinsic parameters, expressed as a 3×3 matrix K to the imaging geometry as well as the extrinsic parameters which determinate the camera's translation and rotation movement in relation to the robot coordinate system. The extrinsic parameters are determined by robot eye-to-hand calibration, more specifically, to solve a homogeneous matrix equation of the form $AX = XB$ and obtain the transformation matrix T .

Finally, the detected and located information in the image plane will be transformed to 3D world coordinates, it is noted that we calibrate the probe magazine plane to camera based on the structured work environment here.

III. PRINCIPLE OF VISION DETECTION ALGORITHM

In this section, the detailed vision detection algorithm of the system is discussed, mainly consists of the introduction of image acquisition model, the image enhancement algorithm, local line and arc segments detection based on LSD and the feature segments connection with a verification process.

A. Image acquisition model

Generally, based on the classic Lambertian reflectance [13], image acquisition model can be considered as the multiplication of the illumination and the reflectance. An optical image $f(x, y)$ can be defined as:

$$f(x, y) = i(x, y) r(x, y) \quad (1)$$

where $i(x, y)$ indicates illumination component, characterizing the amount of source illumination incident on the scene, and $r(x, y)$ is the reflectance component of the objects.

B. Image enhancement based on modified HF

Image acquisition model reveals that the reflection component means the features of object itself, the intensity of $i(x, y)$ changes slower than $r(x, y)$ in this model, then $i(x, y)$ is considered to have more low frequency components than $r(x, y)$. Using this fact, we can reduce the significance of illumination component by reducing the low frequency components of the image to overcome the adverse effect of complex illumination variations on edge detection and feature extraction.

Homomorphic filtering (HF) [5] is a popular method used to enhance or restore the degraded images with uneven

illumination by simultaneously normalizing the brightness across an image and increasing contrast. Based on this, low frequency component reduction can be achieved by executing the filtering process in the frequency domain. Eq. 1 can be converted into a linear model by using the log operation and then transformed from spatial domain to frequency domain applied by discrete Fourier transform:

$$F(u, v) = I(u, v) + R(u, v) \quad (2)$$

Typical filters for HF process are high pass filters [14] such as Difference of Gaussian (DoG) filter, designed to reduce the low frequency components in frequency domain. HF with high pass filter achieves the enhanced effect under low illumination condition, however, may not appropriate to high illumination condition since normalizing the brightness may perform poor robustness to noise or fake contour for edge detection, as shown in Fig. 3(b). For single channel optical image, uneven strong background illumination may split and destroy the coherence of contour information, especially for the end-face of tube-shaped object (Fig. 3(a)).

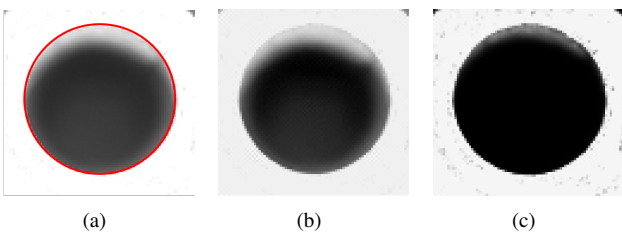


Fig. 3: Partial probe end-face image under high illumination condition. (a) the origin image and expected contour. (b) the result of HF. (c) the result of proposed method.

To solve this problem, we design a frequency gain constrained filter $H(u, v)$ with a control matrix K_c to implement that HF with high pass filter for low illumination condition to increase contrast, as well as HF with low pass filter for high illumination condition to restrain noise and fake contour for edge detection, denoted as the following equations:

$$H(u, v) = \begin{bmatrix} 1 - h(u, v) & h(u, v) \end{bmatrix} K_c \begin{bmatrix} \gamma_H \\ \gamma_L \end{bmatrix} \quad (3)$$

$$h(u, v) = e^{-c[D^2(u, v)/D_0^2]} \quad (4)$$

$$K_c = \begin{bmatrix} k_l & k_{e_1} \\ k_r & k_{e_2} \end{bmatrix} \quad (5)$$

where constant c is used to control the steepness of the slope, D_0 is the cut-off frequency, $D(u, v)$ is the distance between coordinates (u, v) and the centre of frequency, γ_H is the high frequency gain, and γ_L is the low frequency gain. The control matrix K_c is a 2×2 matrix while k_{e_1} and k_{e_2} are regular terms. To reduce the adverse effect of filter applied

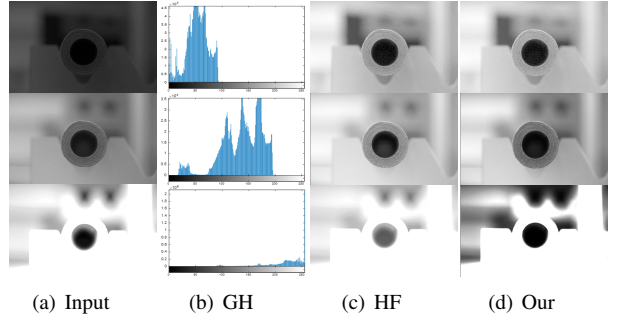


Fig. 4: Image enhanced results under different illumination conditions. The first column is the original image. From the second column to the fourth column: gray histogram, homomorphic filtering, our method.

to high illumination condition, control coefficients k_l and k_r is designed to adjust the filter, denoted as:

$$k_l = \lambda_l M_l + b_l = \lambda_l \left(\sum_{p_{l1}}^{p_{l2}} f_{HG}(x) \right) / S + b_l \quad (6)$$

$$k_r = \lambda_r M_r + b_r = \lambda_r \left(\sum_{p_{r1}}^{p_{r2}} f_{HG}(x) \right) / S + b_r \quad (7)$$

where $f_{HG}(x)$ is the image gray histogram, p_{l1} and p_{l2} are left interval boundaries of gray value keypoints, while p_{r1} and p_{r2} are right interval boundaries. S represents total number pixels of ROI window. λ_l and λ_r are coefficients, b_l and b_r are bias to prevent the case that k_l and k_r appears to 0.

Control coefficients k_l and k_r mainly constraint the form of filter through the pixel proportion in interval (p_{l1}, p_{l2}) named M_l , and the pixel proportion in interval (p_{r1}, p_{r2}) as M_r . To be specific, when illumination is low, M_l greater than M_r and take significant in K_c , the result will be a high pass filter and lead a simultaneous dynamic range compression and contrast enhancement, in contrast, will reduce the effect above, but also bring down the adverse result of fake contour, as shown in Fig. 3(c).

Afterward, returning frequency domain back to spatial domain through inverse discrete Fourier transform to get the filtered image, expressed by the following equation:

$$g(x, y) = \mathfrak{I}^{-1} \{ H(u, v) I(u, v) + H(u, v) R(u, v) \} \quad (8)$$

The enhanced image $g(x, y)$ compared with the original image shown in Fig. 4. We use gray value keypoints constrained filter to replace the high pass filter in homomorphic filtering, which works well under different illumination conditions (Fig. 4(d)) and restores the degraded images robust to fake contour caused by high illumination.

C. Local line and arc segments detection

Line Segment Detector (LSD) [11] is a robust linear-time segment detector algorithm that works through growing region of points with aligned Level Line Angle θ_{LLA} and verified by region's Number of False Alarms (NFA). Each

line support region (a set of pixels) is a candidate for a line segment, and the corresponding geometrical object must be associated with it, which means LSD algorithm demands the independence between pixels when conducting gradient computation. LSD connects pixels with similar gradient level line angles with region growing method, the similar gradient level line angle threshold denoted as the *region angle* θ_{region} and each time a pixel is added to the region, θ_{region} is updated to:

$$\theta_{region} = \arctan \left(\frac{\sum_j \sin(\theta_{LLA_j})}{\sum_j \cos(\theta_{LLA_j})} \right) \quad (9)$$

Finally, each line segment is validated based on a *contrario* model and the Helmholtz principle proposed by Desolneux et al. [15]. The region's NFA is defined as:

$$NFA(r) = (NF)^{5/2} \gamma \sum_{j=k}^n \binom{n}{j} p^j (1-p)^{n-j} \quad (10)$$

where r is the $M \times N$ rectangle region, n is the total number of pixels in the rectangle, a total of γ different values for precision p are tried, and the number of *p-aligned* is denoted by k . The rectangles with $NFA(r) \leq \varepsilon$ are validated as detection results where ε is NFA threshold.

LSD is used to detect low-level line segment feature, however, arc feature is also fundamental feature in object detection. A modified LSD algorithm named arc-support line segment detector is used to extract arc feature in the edge image proposed by Lu. et al. [12], unlike LSD that detects all the LSs, it only detects the arc-support LSs whose distribution changes like a curve. For two terminals of the circumscribed rectangle of the support region are A and B , the central point of the arc-region is C , the *arc-region angle* is denoted as:

$$\theta_{arc-region} = \arctan \left(\frac{\sum_{p_j} \sin(\theta_{LLA_{p_j}})}{\sum_{p_j} \cos(\theta_{LLA_{p_j}})} \right) \quad (11)$$

where p_j belongs to arc-region and the main angle of the arc-support region is denoted as $\angle \overrightarrow{AB}$, the main angles of two sub-regions $\angle \overrightarrow{AC}$ and $\angle \overrightarrow{CB}$ can be obtained through the equation above.

D. Feature segments connection and verification

Local feature detected above contains thousands of low-level line and arc segments, however, are likely to be fragmented due to the constraints of region growing method. To form the integrated line feature or circle feature, we need to connect the local fragmented feature segments.

For detected line segments, since LSD is based on level line field that the line segment added to the region if its' level-line angle is equal to the region angle θ_{region} up to a tolerance τ , but for the intersection parts or the discontinuous points which may be influenced by noise or bad edge, the

direction of gradient differs between segments and the level-line angle difference beyond the threshold, thus can not be clustered together and aligned as expected. The method we used to connect split line segments combines computational geometry and empirical criterion that the two line segments should nearly be collinear and their terminals are close to each other.

The criteria is implemented as Fig. 5 shows, taking two non-intersect line segments LS_i and LS_j respectively, the terminals of LS_i are point A and B , while for LS_j are point C and D . Two line segments are defined close to each other if the distance of a terminal point in LS_i to one terminal point of LS_j less than a tolerance τ_c . We test whether the acute angle between connected line segment of midpoint and LS_i , labeled as α_{ij} , and the acute angle between connect line segment of midpoint and LS_j , labeled as β_{ij} are both less than a certain tolerance angle θ_τ , as the following equation:

$$\max(\alpha_{ij}, \beta_{ij}) \leq \theta_\tau \quad (12)$$

Besides, for each new line segment added to the current merged line segment, we need to test the two properties of the new line segment with every line segment part in the current merged line segment to keep off the curve merged problem as Fig. 5 shows. In the meantime, we update the bigger one of α_{ij} and β_{ij} as the current acute angle.

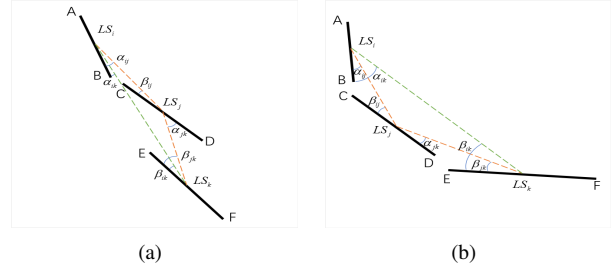


Fig. 5: Separated line segments connect situations. (a) a feasible connect example. (b) an unfeasible example.

For detected arc-support segments, according to the paired line segments analysis of Lu.'s method, Most of the pairs will not contribute to merging the same circle since there is a high probability that two arc-support LSs come from different circles or curves. To verify whether arc-support LSs pairs $\{aLS_i, aLS_j\}$ belong to the same circle or curve, the radius of curvature of aLS_i and aLS_j denote as R_i and R_j should be within a radial distance tolerance ε_{rd} .

Fragmented arc-support segments clustered by Lu.'s method achieve good results under normal illumination condition, however, high illumination added to the end-face of tubular object will rise the circle contour partially incomplete problem, as Fig. 6 shows, the set of arc-support LSs $\{l_{f1}, l_{f2}, \dots, l_{fm}\}$ are not the true contour of target in the real world but the edge of the shadow which is projected inside the probe tube due to external strong illumination,

denoted as fake contour, and the corresponded real contour set is $\{l_{r1}, l_{r2}, \dots, l_{rn}\}$. As observed, the curvature of fake contour less than real contour, in this case, a pair restriction added as the following equation:

$$\rho_{arc_i} < k_f \bar{\rho}_f + k_r \bar{\rho}_r \quad (13)$$

where ρ_{arc_i} is the radius of curvature of i th arc-support segment, $\bar{\rho}_f$ and $\bar{\rho}_r$ are the mean value of the radius of two set above respectively, k_f and k_r are coefficient parameters, segment if not satisfy the restriction will be eliminated.

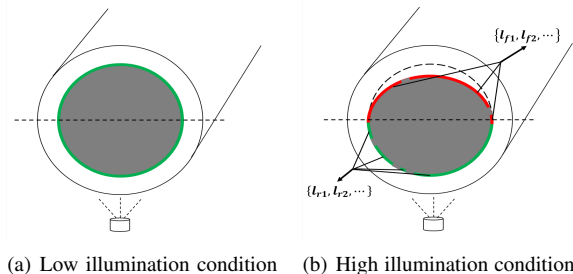


Fig. 6: Single direction illumination condition for probe end-face (green curves are true contour, while red ones represent fake contour). (a) contours under low illumination conditions. (b) contours under high illumination condition.

In fact, the initial circles generated from the valid pairs of arc-support LSSs have many duplicates, therefore, non-maximum suppression via mean-shift clustering [16] applied to remove the duplicates. The candidate sets of arc-support LSSs are fitted using least-squares fitting and verified by a series of steps of validation. Firstly, $2\pi R\sigma_n$ valid edge pixels on the circle are required with a ratio threshold σ_n . Then, the completeness of the fitted circle is also an important criterion, since the fake contour generated by high illumination contribute less to the circle fitted by true contour, the angular coverage of the circular connected component of edge pixels are measured with completeness at least σ_{ac} degrees, generally less than 180° under this circumstance. Recall that fake contour may contributes to generating a circle, the circles generated by fake contours and true contours are partly overlapped, we measure the overlap area S_{ol} of circle generated by same pair arc-support LSSs, and calculate the proportion to the correlated circle, denoted as P_f and P_r respectively, and accept the high proportion one. In addition, for the structured work environment, the radius of the circle candidates can be restricted in a certain range with boundary R_l and R_h . The constraint is denoted as:

$$\begin{cases} N_i > 2\pi R\sigma_n \\ \theta_i > \sigma_{ac} \\ R_l < R_i < R_h \end{cases} \quad (14)$$

where N_i is the valid edge pixels of i th circle candidate, θ_i is the angular coverage, and R_i is the radius.

After extracting and detecting the line or circle feature of the target, we can fit the feature twice as Lu.'s method mentioned, since a candidate after the first line or circle fitting generate the final feature, the new inliers are more sufficient than the old. Hence, twice fitting confirms the final target localization information.

IV. EXPERIMENTS

In this section, we describe the experiment to test the accuracy and robustness of the proposed vision detection system.

We compare our method with two classic methods namely template matching (TM) and Circle Hough Transform (CHT), as well as Lu.'s method in [12]. We use photoelectric sensor to measure the ground truth position of the probe end-face in the calibration plane generally constrained in the probe magazine plane, to compare with the detection results.

For experiment evaluation, we prepare a dataset of industrial probe end-face image, divided into three subsets of low illumination condition named subset A (148 images), normal illumination condition subset B (170 images) and high illumination condition subset C (126 images). In addition, the dataset includes uniform and uneven illumination conditions.

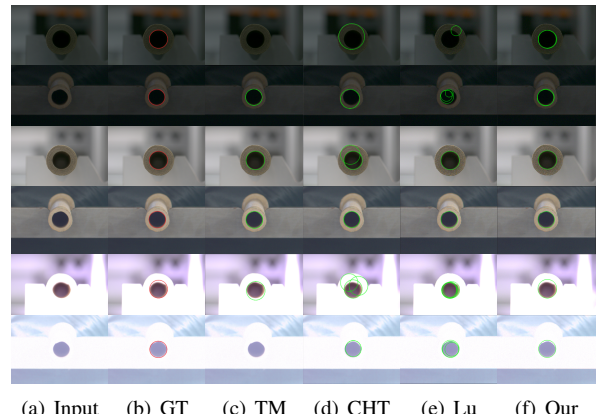


Fig. 7: Detection results under different illumination conditions. From the first row to the last row, every two rows represent different illumination conditions, respectively low, normal and high. The first column is the original image, the second column is the manually annotated ground truth (GT). From the third column to the sixth column: TM, CHT, Lu.'s method, our method.

Fig. 7 illustrates some examples from the probe end-face image dataset, note that the radius of detected results are limited less than a threshold. In general, shape-based TM and CHT are widely used in industrial machine vision with nearly constant illumination condition. As we can see, under normal illumination condition, TM and the method proposed by Lu et al. [12] can detect true results (TPs) and

not cause false positives (FPs), but CHT causes some FPs. However, for low or high illumination condition, TM may lose effectiveness on true circle feature detection, namely false negatives (FNs), while as for CHT, the results are mainly FPs. The method proposed by Lu et al. [12] shows a limited robustness on complex illumination conditions and can detect TPs especially on high illumination condition, but also contains some FPs. On the contrary, our method performs well on different illumination condition and shows strong robustness due to the process of image enhancement and modified arc-support LSs detection method as Fig. 7(f) shows.

TABLE I: Results in the probe end-face image dataset

Dataset	Index	CHT	Lu	Our
Subset A		0.3108	0.4797	0.8108
Subset B	Detection rate	0.8529	0.9824	0.9882
Subset C		0.4762	0.8968	0.9365
Probe Dataset	Error/mm	1.287	0.680	0.413
	Time/s	1.672	0.446	0.841

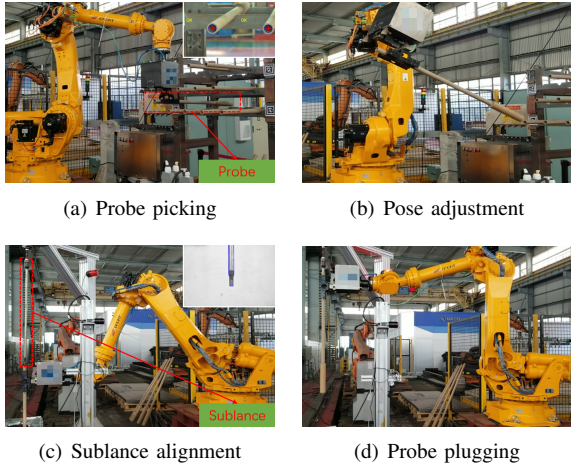


Fig. 8: Peg-hole assembling technological process. (a) Probe picking from magazine based on the detected results. (b) Robot pose adjustment. (c) Sublance and probe alignment. (d) Probe plugged to finish the peg-hole task.

Detailed comparison results are showed in Table I. Note that we measure the localization error use a photoelectric sensor just for the detected TPs result with the horizontal direction paralleling to the camera coordinate system. Also, since TM needs a series of templates in our experiment, so we will not compare here. The results indicate that the detection rate and localization error of the proposed method herein is much better compared to CHT and the method in [12], however, since the image enhancement process is less efficient, the average time of our method is inferior to the method in [12]. In addition, we perform the peg-hole assembling task experiment based on the detected and located results of the vision detection system as Fig. 8 shows.

V. CONCLUSION

In this paper, we proposed a vision detection system for object detection and localization under complex illumination conditions for industrial robot applications, the algorithm mainly use homomorphic filtering with a frequency gain constrained filter to enhance the image, and detect the line and circle feature based on LSD and arc-support LSs. The experiment shows the robustness and effectiveness of the proposed method on the probe end-face image dataset, which can be considered to apply to industrial vision-based applications such as steelmaking automation manufacture.

REFERENCES

- [1] Kaifu Zhang, Yihui Li, Yisheng Guan, Li He, Yuxi Gan, and Zhenjiang Dong. A vision detection system for odd-form components. In *2018 IEEE International Conference on Robotics and Biomimetics (ROBIO)*, pages 120–125. IEEE, 2018.
- [2] Daniel J Jobson, Zia-ur Rahman, and Glenn A Woodell. A multiscale retinex for bridging the gap between color images and the human observation of scenes. *IEEE Transactions on Image processing*, 6(7):965–976, 1997.
- [3] Weilong Chen, Meng Joo Er, and Shiqian Wu. Illumination compensation and normalization for robust face recognition using discrete cosine transform in logarithm domain. *IEEE Transactions on Systems, Man, and Cybernetics, Part B (Cybernetics)*, 36(2):458–466, 2006.
- [4] Yinan Yu, Kaiqi Huang, Wei Chen, and Tieniu Tan. A novel algorithm for view and illumination invariant image matching. *IEEE transactions on image processing*, 21(1):229–240, 2011.
- [5] Su-Ling Lee and Chien-Cheng Tseng. Image enhancement using dct-based matrix homomorphic filtering method. In *2016 IEEE Asia Pacific Conference on Circuits and Systems (APCCAS)*, pages 1–4. IEEE, 2016.
- [6] John Canny. A computational approach to edge detection. *IEEE Transactions on pattern analysis and machine intelligence*, (6):679–698, 1986.
- [7] Dana H Ballard. Generalizing the hough transform to detect arbitrary shapes. *Pattern recognition*, 13(2):111–122, 1981.
- [8] ER Davies. A modified hough scheme for general circle location. *Pattern Recognition Letters*, 7(1):37–43, 1988.
- [9] Teh-Chuan Chen and Kuo-Liang Chung. An efficient randomized algorithm for detecting circles. *Computer Vision and Image Understanding*, 83(2):172–191, 2001.
- [10] Jianke Chen, Chao Hu, Xiaoying Yuan, Zhongqing Feng, and Houxiang Miao. An identification and classification method for circular object based on rotating image template matching. In *2013 IEEE International Conference on Mechatronics and Automation*, pages 1338–1343. IEEE, 2013.
- [11] Rafael Grompone Von Gioi, Jeremie Jakubowicz, Jean-Michel Morel, and Gregory Randall. Lsd: A fast line segment detector with a false detection control. *IEEE transactions on pattern analysis and machine intelligence*, 32(4):722–732, 2008.
- [12] Changsheng Lu, Siyu Xia, Wanming Huang, Ming Shao, and Yun Fu. Circle detection by arc-support line segments. In *2017 IEEE International Conference on Image Processing (ICIP)*, pages 76–80. IEEE, 2017.
- [13] Yong Cheng, Liangbao Jiao, Xuehong Cao, and Zuoyong Li. Illumination-insensitive features for face recognition. *The Visual Computer*, 33(11):1483–1493, 2017.
- [14] Jim R Parker. *Algorithms for image processing and computer vision*. John Wiley & Sons, 2010.
- [15] Agnes Desolneux, Lionel Moisan, and Jean-Michel Morel. *From gestalt theory to image analysis: a probabilistic approach*, volume 34. Springer Science & Business Media, 2007.
- [16] Yizong Cheng. Mean shift, mode seeking, and clustering. *IEEE transactions on pattern analysis and machine intelligence*, 17(8):790–799, 1995.